International Journal of Chemical Studies

P-ISSN: 2349–8528
E-ISSN: 2321–4902
IJCS 2016; 4(5): 59-62

Received: 13-07-2016
Accepted: 14-08-2016

Hem Raj Pant
Engineering Science and Humanities Department, Pulchowk Campus, Tribhuvan University, Kathmandu Nepal

Correspondence
Hem Raj Pant
Engineering Science and Humanities Department, Pulchowk Campus, Tribhuvan University, Kathmandu Nepal

Facile fabrication of highly porous electrospun TiO_2 nanotube and its photocataltytic application

Hem Raj Pant

Abstract
In this work porous, hollow TiO_2 fibers were fabricated using modified coaxial nozzle electrospinning set-up from a polymer sol-gel solution of $CaCO_3$ and TiO_2 precursor. Two solutions, a TiO_2 precursor containing polyvinyl acetate (PVAc) solution with a small amount of $CaCO_3$ and PVAc solution with a sufficient amount of $CaCO_3$, were separately passed through the outer and inner nozzles, respectively. Hollow, porous TiO_2 nanofibers were obtained by etching $CaCO_3$ on calcined TiO_2 fibers using dilute HCl. Field emission scanning electron microscopy images revealed that the as-fabricated TiO_2 fibers were nanotubes with porous walls. Such a highly porous TiO_2 nanotubes exhibited higher photocatalytic activities toward degradation of Rhodamine B in comparison to the other nanostructured TiO_2 materials such as commercial P25 nanoparticles and regular TiO_2 nanofibers.

Keywords: TiO_2; Nanotubes; Coaxial electrospinning

1. Introduction
Semiconductor titanium dioxide (TiO_2) has been reported as one of the most attractive materials for researchers during the last few decades [1-3]. Research works of different groups have led to the formation of effective one-dimensional TiO_2 structures (nanofibers, nanotubes, nanowires, nanorods, and nanobelts) that exhibit remarkable characteristics due to their exceptional geometry [4]. The electrospinning technique is a widely used technique for producing fibers including polymer and organic/inorganic hybrids [5]. Electrospinning followed by calcination is one of the most applied facile techniques for the fabrication of TiO_2 nanofibers using a blend of TiO_2 precursor and polymer solution [6]. Due to potential applications in photocatalysis the hollow structure with a large number of pores, high surface area, chemical inertness, and good mechanical stability have drawn considerable attention [7-10].

Xiang Zhang *et al*. fabricated hollow, 1D, porous TiO_2 nanofibers by coaxial electrospinning of a titanium tetraisopropoxide (TTIP) solution with two polymers solution, using a core–shell spinneret, followed by annealing at 450 °C [11]. He *et al*. reported the fabrication of hollow/tubular TiO_2 NFs from coaxial electrospinning using paraffin oil in the inner nozzle and a precursor containing PVP solution in the outer nozzle [4]. However, this process could not produce sufficient pores on the nanotube walls [12].

Here we fabricated multifunctional porous nanotubes $CaCO_3$. When $CaCO_3$-containing TiO_2 nanofibers were treated with dilute HCl, nearly all of the $CaCO_3$ was etched out to introduce pores to the TiO_2 nanofibers.

Different reports describe that such a hollow porous TiO_2 nanofibers demonstrate faster electron diffusion, and longer electron recombination time than regular TiO_2 nanofibers as well as p25 nanoparticles [13]. Therefore, calcinations of composite nanofibers obtained from the coaxial electrospun nanofibers made by using the precursor of TiO_2 and $CaCO_3$ nanoparticles after the acid treatment can produce highly photocatalytic hollow porous TiO_2 nanotubes.

2. Experimental Section
Titanium isopropoxide (TIP) from Junsei Co. Ltd., Japan, Polyvinyl acetate (PVAc, Mw = 500,000) from Sigma-Aldrich (USA), and calcium carbonate were used to fabricate porous TiO2 nanotubes. PVAc solution (20 wt%) containing 20 wt% CaCO3 (with respect to polymer) was prepared by dissolving PVAc in DMF solvent under magnetic stirring for 12 h.

5 g of TIP was taken in a separate bottle followed by drop wise addition of acetic acid to get transparent solution. Then 6 g of as-prepared PVAc solution was added to this solution with vigorous stirring for 30 min. This solution was placed in a syringe connected to the outer capillary of a coaxial spinneret while 20 wt% PVAc solution containing 50 wt% CaCO3 with respect to polymer (without TIP) was placed in another syringe connected to the inner capillary. TiO2 NFs from single nozzle were fabricated from the mixture of 6 g 20 wt% PVAc solution and 5 g of as-prepared TIP solution. Electrospinning was carried out at an applied voltage of 17 kV, tip-to-collector distance of 18 cm, and a solution feed rate of 1 ml/h at room temperature. Temperature and humidity were 28% and 39%, respectively. As-fabricated electrospun nanofibrous mats were placed in vacuum being dried for 12 h at 30 °C. Finally these fibers were calcined at 500^{O}C for three hour to remove the polymer. TiO2 fibers were labeled STiO2, CTiO2, and HTiO2 for pure TiO2 fibers obtained from single nozzle, CaCO3/TiO2 fibers obtained from coaxial nozzle, and HCl treated porous TiO2 nanotube, respectively.

2.1 Characterizations

The surface properties of the $STiO_2$, $CTiO_2$, and $HTiO_2$ fibers were characterized by field emission scanning electron microscopy (FE-SEM; Hitachi S-7400, Hitachi Co., Tokyo, Japan) and high resolution transmission electron microscopy (TEM, JEM-2010, JEOL, Japan). The composition of the prepared fibers was analyzed through X-ray diffraction (XRD, Rigaku, Japan) with Cu Kα (λ = 1.540 Å) radiation of Bragg angles ranging from 20 to 80°.

2.2. Photocatalytic activity

The photocatalytic activities of P25, $STiO_2$, and $HTiO_2$ were evaluated by degradation of an aqueous Rhodamine B (RhB) solution (10 ppm) under mild UV irradiation at room temperature. Experiment was carried out in a 100 ml beaker equipped with a light guide (5 mm diameter) connected to a mercury vapor lamp (Omni cure, EXFO). The distance between the light guide and the solution was maintained at 5cm. In a typical experiment, 0.02 g of powdered samples was mixed with 30 ml of RhB solution. Before irradiation, samples and dye solution mixture was made homogeneous by stirring for 30 min in the dark and also to achieve adsorption-desorption equilibrium. After then, the sample was irradiated with UV light and 1 ml of the sample was withdrawn from the solution at defined time intervals. Residual catalyst from the withdrawn samples was separated by centrifuging, and the RhB concentration in the suspension was observed using a UV-visisble spectrophotometer (HP 8453 UV–visible spectroscopy system, Germany) at the corresponding wavelength. The remaining RhB concentration (%) after various intervals of time could be estimated by the following equation:

$$\text{Degradation efficiency (\%)} = \left(1 - \frac{C}{C_0}\right) * 100\%$$

Where $C_\circ$ is initial concentration and C is the concentration after "t" minute of light irradiation. The stability of the catalyst was also performed by degrading the same ppm RhB solution.

3. Results and discussion

3.1. Morphology

The morphologies of the fibers before calcination are shown in Figure 1. Figures 1a and 1b show the fiber morphology of TiO_2 NFs from a single nozzle and coaxial nozzle before calcination, respectively. As shown in Figure 1b, the diameter of the fibers from the coaxial nozzle was larger than those from the single nozzle, which corresponds to the results of $CaCO_3$ content. Figure 1C shows the TEM images of electrospun fibers.

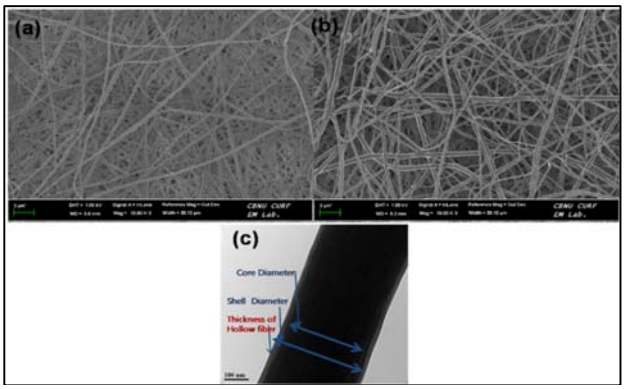

Fig 1: FE-SEM images of (a) TiO_2 NFs from single nozzle and (b) $CaCO_3/TiO_2$ NFs from coaxial nozzle before calcinations and (c) TEM image of TiO2 fiber.

As shown in Figure. 2, the $STiO_2$ fibers obtained from the TIP/PVAc blend solution using single-nozzle electrospinning were continuous with a non-porous wall (Figure. 2a). Coaxial electrospinning of the $CaCO_3$/PVAc core and $CaCO_3$-TIP/PVAc shell introduced a certain surface roughness to the $CTiO_2$ NFs (Figure. 2b). Due to it high reactivity with dilute HCl, nearly all of the $CaCO_3$ should be etched from the fiber during acid treatment pores will be created. Since the core portion is enriched in $CaCO_3$, whereas the shell portion is enriched in TiO_2, the core becomes hollow (tube-like structure) and the wall of the tube becomes highly porous. FE-SEM images (Figure. 2c).

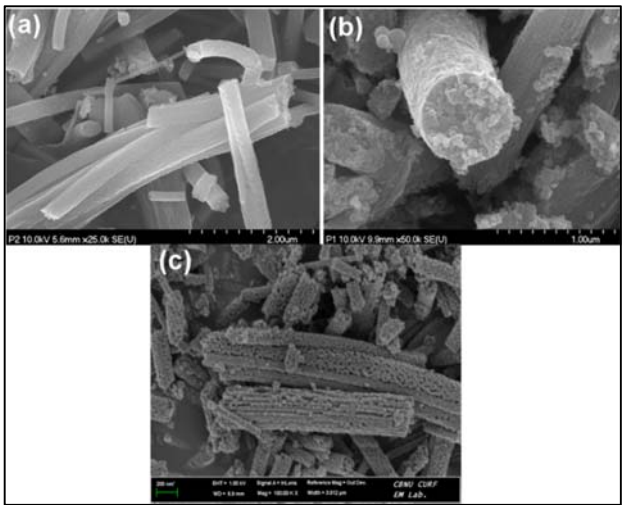

Fig 2: FE-SEM images of (a) TiO_2 NFs from single nozzle (b) $CaCO_3/TiO_2$ NFs from coaxial nozzle, and (c) HCl treated $CaCO_3/TiO_2$ NFs (porous nanotube)

3.2. Crystal Structure

The incorporation of $CaCO_3$ through calcined TiO_2 NFs and the formation of anatase TiO_2 NFs with a minor rutile fraction were further confirmed by XRD analysis. XRD analysis demonstrated the characteristic reflections for calcite with scanning angles of 23.1 (012), 29.6 (104), 36.1(110), 39.48 (113), 43.24 (202), 47.6 (018), and 48.1 (116) of $CaCO_3$ [14, 15]

in the composite fibers. Figure 3 shows the XRD pattern of the acid-treated porous TiO_2 nanotubes, and the diffraction peaks were indexed to (101), (004), (200), (211), and (204) crystallographic planes of the anatase phase of TiO_2 with (110) crystallographic planes of the minor fraction of the rutile phase TiO_2 (PDF card 77-0441 JCPDS) [16].

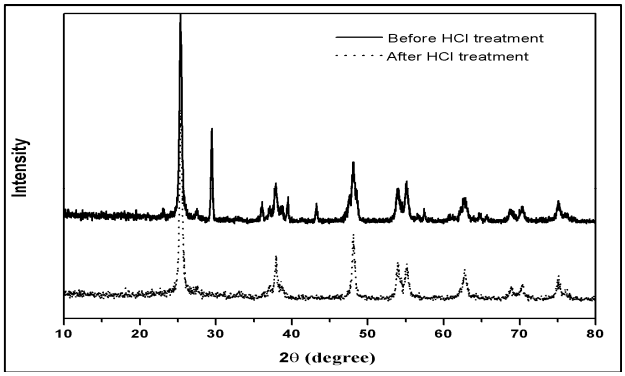

Fig 3: XRD patterns of composite nanofibers before and after dilute HCl treatment.

3.3. Photocatalytic Applications

Figure 4 displays the evolution of the corresponding UV-Vis spectra with UV exposure time. The blank test showing that the self-decomposition of RhB can be neglected in comparison with the photocatalytic performance caused by catalyst particles. From figure it was cleared that after 50 min UV irradiation, almost 100% of the RhB molecules were decomposed by the HCl treated porous and hollow nanotubes ($HTiO_2$) whereas, at the same time, pure TiO_2 fibers obtained from single nozzle ($STiO_2$), decomposed amount of RhB molecules was less than 80%. Photocatalytic performance of P25 was also tested to compare with photocatalytic activity of $HTiO_2$ and $STiO_2$. When P25 was used as the photocatalyst, around 85% of the RhB molecules were decomposed after 50 min. Thus result shows that $HTiO_2$ has better performance than P25 and $STiO_2$. Due to the high specific surface area of the tubular porous nanostructure, high photocatalytic activity is expected from the $HTiO_2$.

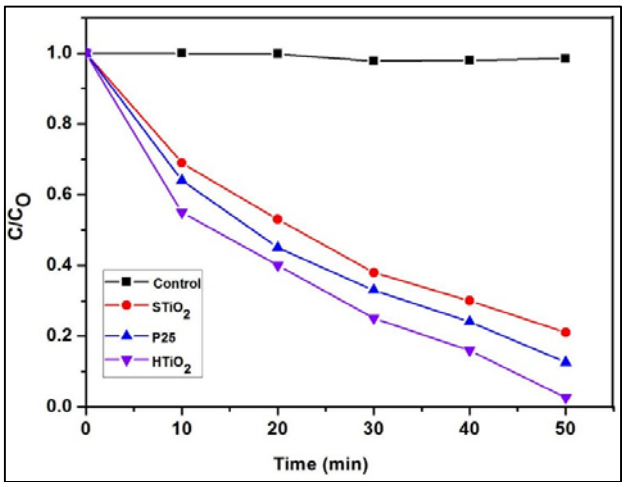

Fig 4: Comparison of photodegradation using different photocatalysis under UV light

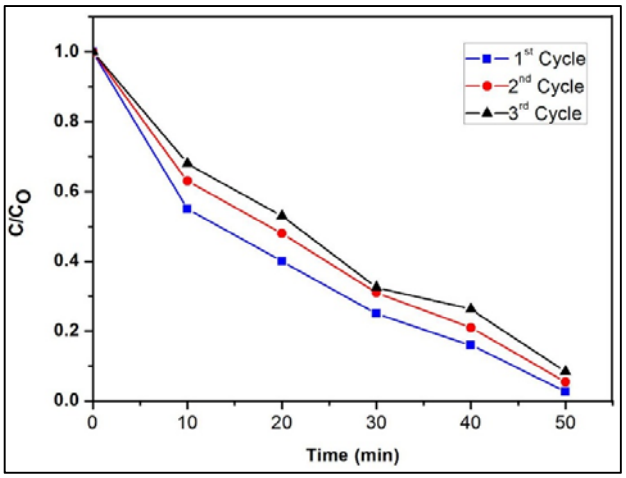

Fig 5: Stability test of HTiO2 nanofibers up to three cycles

Moreover, the stability of the $HTiO_2$ catalyst was examined for the degradation of RhB, which is an important parameter for the practical application. In the reusability test, recovered sample was centrifuged, filtered, and dried in oven at 60^0c for 24 h. This dried sample was then weighed, making the lost portion and used for the next run. Same procedures were used for each cycle. Figure 5 shows the stability of the photocatalys is slightly attenuated after three consecutive photocatalytic experiments but still has high photocatalytic performance.

4. Conclusion

Porous TiO_2 hollow fibers were prepared by coaxial electrospinning and subsequent calcination and acid treatment. Dilute HCl treatment of $CaCO_3/TiO_2$ composite fibers easily produced highly-porous TiO_2 nanotubes. Such a highly-porous TiO_2 nanotube showed enhanced photocatlytic activities under UV light than TiO_2 nanofibers and P25.

5. Acknowledgment

This work was supported by Prof Cheol Sang Kim, Chonbuk National University, South Korea.

6. References

1. Linsebigler ALG, Lu JT, Yates, Photocatalysis on TiO2 Surfaces: Principles, Mechanisms, and Selected Results, Chem. Rev. 1995; 95:735-758.
2. Vu D, Li Z, Zhang H, Wang W, Wang Z, Xu X *et al.* Adsorption of Cu(II) from aqueous solution by anatase mesoporous TiO2 nanofibers prepared via electrospinning, J. Colloid Interface Sci. 2012; 367:429-435.
3. Hu H, Zhang W, Qiao Y, Jiang X, Liu X, Ding C. Antibacterial activity and increased bone marrow stem cell functions of Zn-incorporated TiO2 coatings on titanium, Acta Biomaterialia. 2012; 8:904-915.
4. He G, Cai Y, Zhao Y, Wang X, Lai C, Xi M *et al.* Electrospun anatase-phase TiO2 nanofibers with different morphological structures and specific surface areas, J. Colloid Interface Sci. 2013; 398:103-111.
5. Li D, Xia Y. Electrospinning of Nanofibers: Reinventing the Wheel?, Advanced Materials. 2004; 16:1151-1170.
6. Hou H, Wang L, Gao F, Wei G, Zheng J, Tang B *et al.* Fabrication of porous titanium dioxide fibers and their photocatalytic activity for hydrogen evolution,

International Journal of Hydrogen Energy. 2014; 39:6837-6844.
7. Freeman JJ. Active carbon Edited by R. C. Bansal, J.-B. Donnet and F. Stoeckli. Marcel Dekker, New York, 1988, 14-482, US$150.00. ISBN 0–8247–7842–1, J. Chem. Technol. Biotechnol. 1990; 48:240-241.
8. Foley HC. Carbogenic molecular sieves: synthesis, properties and applications, Microporous Materials, 1995; 4:407-433.
9. Kyotani T. Control of pore structure in carbon, Carbon, 2000; 38:269-286.
10. Choi SY, Mamak M, Coombs N, Chopra N, Ozin GA. Electrochromic Performance of Viologen-Modified Periodic Mesoporous Nanocrystalline Anatase Electrodes, Nano Letters, 2004; 4:1231-1235.
11. Zhang X, Thavasi V, Mhaisalkar SG, Ramakrishna S. Novel hollow mesoporous 1D TiO2 nanofibers as photovoltaic and photocatalytic materials, Nanoscale, 2012; 4:1707-1716.
12. Chang W, Xu F, Mu X, Ji L, Ma G, Nie J. Fabrication of nanostructured hollow TiO2 nanofibers with enhanced photocatalytic activity by coaxial electrospinning, Materials Research Bulletin, 2013; 48:2661-2668.
13. Zhan S, Chen D, Jiao X, Tao C. Long TiO2 Hollow Fibers with Mesoporous Walls: Sol−Gel Combined Electrospun Fabrication and Photocatalytic Properties, The Journal of Physical Chemistry B, 2006; 110:11199-11204.
14. Wei H, Shen Q, Zhao Y, Wang DJ, Xu DF. Influence of polyvinylpyrrolidone on the precipitation of calcium carbonate and on the transformation of vaterite to calcite, Journal of Crystal Growth, 2003; 250:516-524.
15. Kırboga S, Öner M. The inhibitory effects of carboxymethyl inulin on the seeded growth of calcium carbonate, Colloids and Surfaces B: Biointerfaces, 2012; 91:18-25.
16. Choi KI, Ho Lee S, Park JY, Choi DY, Hwang CH, Lee IH *et al*., Fabrication and characterization of hollow TiO2 fibers by microemulsion electrospinning for photocatalytic reactions, Materials Letters, 2013; 112:113-116.